Supporting Information for

Dynamics of deep soil carbon – insights from ^{14}C time-series across a climatic gradient

Tessa Sophia van der Voort[1], Utsav Mannu[1,†], Frank Hagedorn[2], Cameron McIntyre[1,3], Lorenz Walthert[2], Patrick Schleppi[2], Negar Haghipour[1], Timothy Ian Eglinton[1]

[1]Institute of Geology, ETH Zürich, Sonneggstrasse 5, 8092 Zürich, Switzerland
[2]Forest soils and Biogeochemistry, Swiss Federal Research Institute WSL, Zürcherstrasse 111, 8903 Birmensdorf, Switzerland
[3]Department of Physics, Laboratory of Ion Beam Physics, ETH Zurich, Schaffmattstrasse 20, 9083 Zurich
[†]New address: Department of Earth and Climate Science, IISER Pune, Pune, India

Contents of this file:

Introduction

This supporting information provides details on the modeling approach used in this paper, contains ancillary data and details on the estimation of petrogenic carbon.

S1 Numerical model in Matlab Environment

The purpose of this section is to explain the necessity of a robust numerical modelling approach for ^{14}C time-series which can be applied ubiquitously in radiocarbon turnover estimates in oceanic and terrestrial reservoirs. **The code that can be employed to do this is freely available with this paper.** Torn et al. (2009) explains that a single measured radiocarbon value collected on the falling art of the bomb-curve yields two estimates of the turnover time. In the case of two time-points, this uncertainty is avoided and a single estimate can be produced. For this reason, time-series radiocarbon can be crucial. Graven et al. (2015) highlighted that owing to continued burning of fossil fuels, the importance of time-series measurements can only increase. In this section, we elaborate on a sensitivity analysis and error propagation analysis. The Matlab numerical optimization runs iterations until the lowest mean-squared error for both time points is reached. There are separate scripts to determine turnover for a single time-point, a time-series and multiple pools.

S1.1 Necessity of numerical approach

The incorporation of atmospheric ^{14}C into the any terrestrial reservoir is inherently time-dependent, and therefore as be solved numerically, as can be proven in the following manner: For the isotopic signature of any reservoir the value of a variable at R_t can be formulated as the following:

$$R_t = R_{t-1} + \frac{\delta R_{t-1}}{\delta t}\Delta t \qquad Eq.SI.1$$

Here R_t refers to the new value, R_{t-1}refers to the previous point, $\frac{\delta R_{t-1}}{\delta t}$ is the derivative (i.e. slope) of the previous point and Δt refers to the time-step between t and $t-1$. For any case of uptake of atmospheric $^{14}CO_2$, the derivative can be determined:

$$\frac{\delta R_{t-1}}{\delta t} = (-\lambda - \kappa)R_{t-1} + \kappa \cdot R_{atm,t} \qquad Eq.SI.2$$

Here, λ refers to the decay rate of ^{14}C, κ to the turnover rate, and $R_{atm,t}$ to the atmosperhic value of the atmosphere of year t. When we combine Eq. SI.1 and Eq. SI.2. Substituting Eq. SI.1 in Eq. SI.2 gives:

$$R_t = R_{t-1} + ((-\lambda - \kappa)\, R_{t-1} + \kappa \cdot R_{atm,t})\Delta t \qquad Eq.SI.3a$$

Which can be rewritten as:

$$R_t = R_{t-1}(1 - \Delta t \cdot \lambda - \Delta t \cdot \kappa) + \kappa \cdot R_{atm,t} \qquad Eq.SI.3b$$

In this particular scenario we have annual data, so Δt can be defined to 1, resulting in:

$$R_t = R_{t-1}(1 - \lambda - \kappa) + \kappa \cdot R_{atm,t} \qquad Eq.SI.4$$

Which equals the Eq. 2.5 provided in Torn et al. (2009). There is an internal inherent dependency of the value of R_t, both dependent on the atmospheric input as well as the previous timepoint, which is also dependent on κ. Therefore, the equation cannot be solved analytically and numerical iteration is required. In the present form, the model can be used in any case for any radiocarbon-based time-series.

S1.2 Comparison with other temporally resolved models

From the scientific literature, we can discern two families of models dealing with temporally resolved datasets that all build on the equations laid out in Torn et al., (2009). Firstly, there is a group that matches the data to excel-based calculations without the help of optimization using atmospheric input data, e.g. in Schrumpf and Kaiser (2015). Our model differs slightly from this as it includes robust error reduction and a non-subjective estimate. Secondly, there is a group which uses the same equations and combine it with the strength of the Excel Solver function (www.solver.com) and error reduction (*Prior et al.*, 2007; *Baisden et al.*, 2013). We will assume that, as the concerned equations of radioactive decay are non-linear, that the non-linear function of the Excel solver function was used. In these cases, two pools are assumed to be present (one fast decadal pool and one slow millennial pool), there is a steady state and the time step is one year. The age of the passive pool is assumed to be constant (e.g. 1000 years) and the spin-up time starts early 19th century, forcing the model to choose a value of the fast pool which is <100 years. The numerical model presented in this study builds on these models by including a measured value of one of the pools instead of an estimated value.

S1.3 Limitations and drawbacks two-pool model

When finding the best fit for a two-pool model, the optimization estimates the values of two unknowns (fraction size and turnover time). Subsequently, the lowest error is searched in a two-dimensional space (fraction size and turnover time). Solving this constitutes an under constrained problem. The error map is illustrated in SI Figure S1. As is shown, the error does converge to a single value, but there are many options which are nearly equally likely – indicating that the result is not very robust. This is opposed to a single-pool model where the error has a single clear lowest point. This limitation should be considered when interpreting these results.

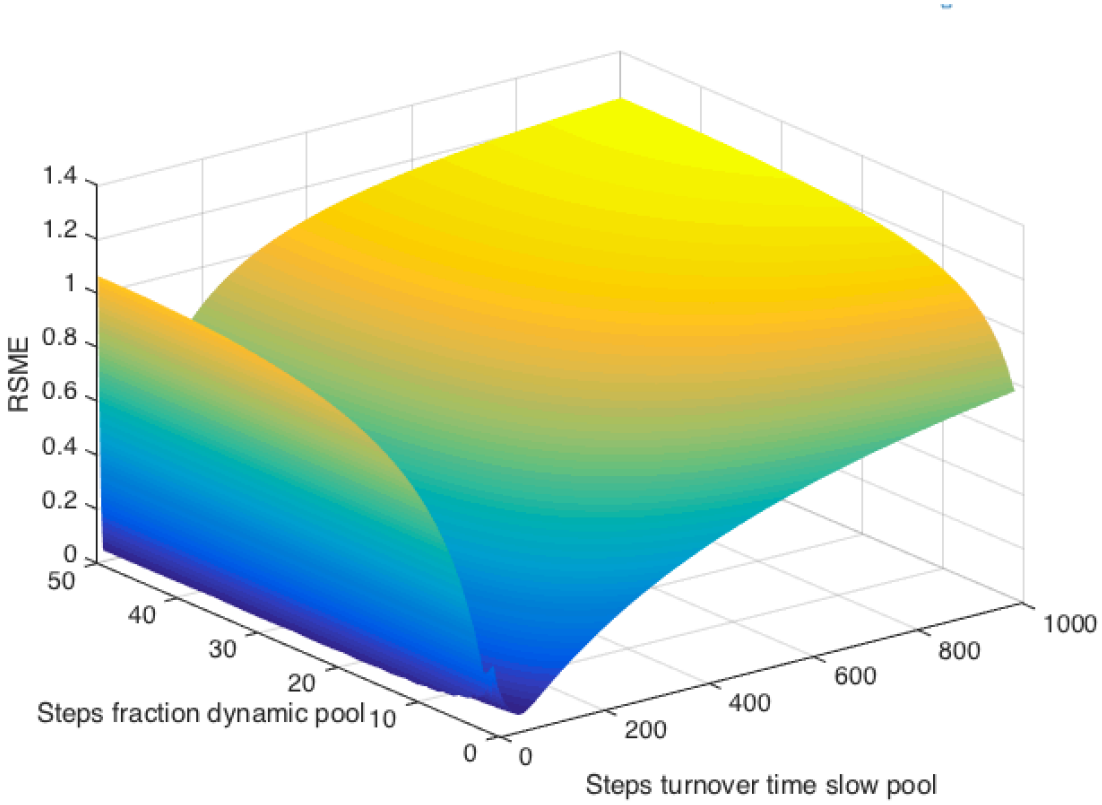

SI Figure 1 Error map of two-pool model for sub-alpine site Beatenberg. The range of turnover times is from 10 to 10.000 in steps of 10, so there are 1000 steps. For the estimated fraction, the range varies from 0.01 to 0.50, so there are 50 steps. The Error is the difference between the modeled R (Equation 3, main text).The pattern *mimics the skewed v-shape as seen for the same sample in a single-pool model (Figure 2), but does not appear very sensitive to the fraction parameter.*

Table S1 Beatenberg $\Delta^{14}C$ data and modelled turnover data, with single- and temporally- resolved radiocarbon data as visualized in Fig. 2.

Average depth (cm)	$\Delta^{14}C$ 1997	$\Delta^{14}C$ 2014	Turnover 1997 (y)	Turnover 2014 (y)	Turnover time-series (y)
Organic layer$_{bulk}$	210.91	98.95	28.7	79.7	14
2.5$_{bulk}$	-17.61	-17.15	404.6	412.8	410
2.5$_{WEOC}$	33.12	7.75	182	199.8	191

Table SI 2 Turnover time (y) for (a) no atmospheric lag and (b) a vegetation-dependent atmospheric lag (Table 2) in the soils of the study sites. Turnover times increase from decadal to centennial in the topsoil to millennial in the deep soil. The modeled vegetation-induced lag only affects the turnover times of the organic layer. As per usual, depth starts at the mineral soil. The organic layer is counted in the negative space. As the organic layer of the Podsol is 20 cm, hence the scale starts at -17.5 cm.

Turnover time without lag

Depth average	Luvisol	Cambisol	Gleysol	Podsol	Fluvisol
-17.50	-	-	-	14	-
-2.50	-	-	-	92.9	-
2.50	78	62	120	410	82
7.50	145	327	198	1175	156
15.00	234	511	715	1656	240
30.00	360	662	2108	1917	615
50.00	1376	1816	4520	1297	608
70.00	3938	1640	4946	-	983
90.00	-	2852	5383	-	-

Turnover time vegetation dependent lag

Depth average	Luvisol - 2 y	Cambisol - 3 y	Gleysol - 7 y	Podsol- 8 y	Fluvisol- 8 y
-17.50	-	-	-	4	-
-2.50	-	-	-	100	-
2.50	80	64	125	404	82
7.50	145	324	200	1169	154
15.00	234	508	714	1651	236
30.00	360	662	2107	1912	607
50.00	1375	1816	4519	1296	607
70.00	3938	1640	4945	-	981
90.00	-	2852	5383	-	-

Table SI 3 Residual error for (a) no atmospheric lag and (b) a vegetation-dependent atmospheric lag (Table 2) in the soils of the study sites.

Residual Error no vegetation lag					
Av. depth (cm)	Othmarsingen	Lausanne	Alptal	Beatenberg	Nationalpark
-17.50	-	-	-	$1.3 \cdot 10^{-2}$	-
-2.50	-	-	-	$3.6 \cdot 10^{-5}$	-
2.50	$2.9 \cdot 10^{-2}$	$6.8 \cdot 10^{-3}$	$1.2 \cdot 10^{-5}$	$7.1 \cdot 10^{-4}$	$5.0 \cdot 10^{-2}$
7.50	$2.0 \cdot 10^{-2}$	$4.1 \cdot 10^{-2}$	$5.9 \cdot 10^{-6}$	$3.6 \cdot 10^{-2}$	$1.9 \cdot 10^{-2}$
15.00	$1.5 \cdot 10^{-3}$	$5.7 \cdot 10^{-2}$	$4.4 \cdot 10^{-6}$	$6.0 \cdot 10^{-2}$	$4.1 \cdot 10^{-3}$
30.00	$1.9 \cdot 10^{-6}$	$6.0 \cdot 10^{-6}$	$1.0 \cdot 10^{-6}$	$6.0 \cdot 10^{-2}$	$4.0 \cdot 10^{-2}$
50.00	$2.2 \cdot 10^{-7}$	$1.7 \cdot 10^{-7}$	$7.9 \cdot 10^{-7}$	$1.3 \cdot 10^{-6}$	$6.9 \cdot 10^{-6}$
70.00	$1.4 \cdot 10^{-1}$	$5.2 \cdot 10^{-7}$	$5.1 \cdot 10^{-8}$	-	-
90.00	-	$2.7 \cdot 10^{-6}$	$1.8 \cdot 10^{-6}$	-	-

Residual Error with vegetation lag					
Av. depth (cm)	Othmarsingen 2 years	Lausanne 3 years	Alptal 7 years	Beatenberg 8 years	Nationalpark 8 years
-17.50	-	-	-	$2.9 \cdot 10^{-2}$	-
-2.50	-	-	-	$1.3 \cdot 10^{-5}$	-
2.50	$3.1 \cdot 10^{-2}$	$1.0 \cdot 10^{-2}$	$1.2 \cdot 10^{-5}$	$2.2 \cdot 10^{-3}$	$4.2 \cdot 10^{-2}$
7.50	$2.1 \cdot 10^{-2}$	$4.0 \cdot 10^{-2}$	$1.1 \cdot 10^{-5}$	$3.6 \cdot 10^{-2}$	$1.5 \cdot 10^{-2}$
15.00	$2.0 \cdot 10^{-3}$	$5.6 \cdot 10^{-2}$	$5.8 \cdot 10^{-6}$	$5.9 \cdot 10^{-2}$	$6.7 \cdot 10^{-3}$
30.00	$9.0 \cdot 10^{-6}$	$7.3 \cdot 10^{-3}$	$1.6 \cdot 10^{-6}$	$5.9 \cdot 10^{-2}$	$3.9 \cdot 10^{-2}$
50.00	$5.8 \cdot 10^{-7}$	$3.5 \cdot 10^{-6}$	$6.4 \cdot 10^{-7}$	$5.7 \cdot 10^{-7}$	$6.2 \cdot 10^{-7}$
70.00	$1.4 \cdot 10^{-1}$	$3.3 \cdot 10^{-6}$	$9.3 \cdot 10^{-7}$	-	$1.3 \cdot 10^{-6}$
90.00	-	$1.9 \cdot 10^{-6}$	$8.4 \cdot 10^{-8}$	-	

Table S4 Overview of the carbon content of the bulk soil and the relative contribution of WEOC to the total organic carbon pool.

	Othmarsingen		Lausanne		Alptal		Beatenberg		Nationalpark	
Av. Depth	Bulk C (%)	WEOC $C^{-1}gsoil^{-1}$ (%)	Bulk C (%)	WEOC $C^{-1}gsoil^{-1}$ (%)	Bulk C (%)	WEOC $C^{-1}gsoil^{-1}$ (%)	Bulk C (%)	WEOC $C^{-1}gsoil^{-1}$ (%)	Bulk C (%)	WEOC $C^{-1}gsoil^{-1}$ (%)
-17.5	-	-	-	-	-	-	34.4	-	-	-
-2.5	-	-	-	-	-	-	27.3	-	-	-
2.5	3.7	$5.4 \cdot 10^{-5}$	5.4	$6.6 \cdot 10^{-5}$	44.8	$1.1 \cdot 10^{-5}$	9.2	$2.4 \cdot 10^{-4}$	21.6	$2.0 \cdot 10^{-5}$
7.5	1.6	$9.5 \cdot 10^{-5}$	1.9	$1.7 \cdot 10^{-4}$	13.5	$6.9 \cdot 10^{-5}$	2.4	$3.1 \cdot 10^{-4}$	7.5	$3.2 \cdot 10^{-5}$
15	1.4	$9.6 \cdot 10^{-5}$	1.4	$1.8 \cdot 10^{-4}$	7.4	$4.6 \cdot 10^{-4}$	2.0	$3.2 \cdot 10^{-4}$	1.7	$1.4 \cdot 10^{-4}$
30	0.9	$1.4 \cdot 10^{-4}$	0.8	$2.4 \cdot 10^{-4}$	5.1	$2.9 \cdot 10^{-5}$	0.6	$3.9 \cdot 10^{-4}$	0.6	-
50	0.3	-	0.5	$5.1 \cdot 10^{-4}$	2.4	-	0.8	$2.9 \cdot 10^{-4}$	0.2	-
70	0.2	-	0.2	$1.1 \cdot 10^{-3}$	3.1	-	-	-	0.2	-
90	-	-	0.2		2.3	-	-	-	-	-

Table S5 Modelled turnover time of bulk carbon, the dynamic WEOC pool and estimates of dynamic pool size and error.

Site	Depth	WEOC turnover (y)	Bulk turnover (y)	Estimated size dynamic pool	Residual error two-pool model
Othmarsingen	2.5	38.4	78	0.2	$1.8 \cdot 10^{-2}$
	7.5	33.4	145	0.15	$6.1 \cdot 10^{-3}$
	15	33.4	234	0.01	$1.7 \cdot 10^{-3}$
	30	33.4	360	-	-
	50	1001	1376	-	-
	70	-	3938	-	-
Lausanne	2.5	31.8	62	0.1	$3.9 \cdot 10^{-3}$
	7.5	80	327	0.01	$4.1 \cdot 10^{-2}$
	15	98.2	511	0.01	$5.7 \cdot 10^{-2}$
	30	185.6	662	-	-
	50	987.4	1816	-	-
	70	1501.9	1640	-	-
	90	-	2852	-	-
Alptal	2.5	42.1	120	-	-
	7.5	111.2	198	-	-
	15	254.6	715	-	-
	30	892.9	2108	-	-
	50	-	4520	-	-
	70	-	4946	-	-
	90	-	5383	-	-
Beatenberg	2.5	191.3	410	0.26	$8.0 \cdot 10^{-4}$
	7.5	282.6	1175	0.41	$3.6 \cdot 10^{-2}$
	15	348.8	1656	0.47	$5.9 \cdot 10^{-2}$
	30	923.2	1917	0.23	$5.9 \cdot 10^{-2}$
	50	431.1	1297	-	-
Nationalpark	2.5	63.9	82	0.01	$5.0 \cdot 10^{-2}$
	7.5	96.3	156	0.01	$1.9 \cdot 10^{-2}$
	15	104.8	240	0.47	$1.3 \cdot 10^{-3}$
	30	213.5	615	0.1	$4.0 \cdot 10^{-2}$
	50	-	608	-	-
	70	-	983	-	-

Table S6 Estimation potential contribution petrogenic carbon for two sites containing sedimentary carbon assuming for Alptal the signature of a sedimentary-carbon free soil and for Lausanne the shallower depth. The signature of the shale is assumed to be devoid of radiocarbon. The fossil contribution = $\frac{\Delta^{14}C_{measurement} - \Delta^{14}C_{non-fossil\ carbon\ soil}}{\Delta^{14}C_{shale} - \Delta^{14}C_{non-fossil\ carbon\ soil}}$

	$\Delta^{14}C_{\text{Alptal at 90 cm}}$ (‰)	$\Delta^{14}C_{\text{Beatenberg at 60 cm}}$ (‰)	Shale (‰)	Contribution fossil
Alptal $\Delta^{14}C_{\text{90 cm}}$ (‰)	-640.3	-421.3	-1000	0.38
		$\Delta^{14}C_{\text{Lausanne at 80 cm}}$ (‰)		
Lausanne $\Delta^{14}C_{\text{145 cm}}$ (‰)	-533.2	-252.5	-1000	0.38
Lausanne $\Delta^{14}C_{\text{210 cm}}$ (‰)	-403.5	-252.5	-1000	0.20
Lausanne $\Delta^{14}C_{\text{270 cm}}$ (‰)	-186.4	-252.5	-1000	-
Lausanne $\Delta^{14}C_{\text{310 cm}}$ (‰)	-820.2	-252.5	-1000	0.76

Table S7 Pedogenic oxides as determined by oxalate-exactable Fe and Al on soil samples on single profiles taken proximal to the plots (courtesy Stephan Zimmerman, WSL LWF).

Othmarsingen			Lausanne			Alptal			Beatenberg			Nationalpark		
Soil depth (cm)	Fe (ppm)	Al (ppm)	Soil depth (cm)	Fe (ppm)	Al (ppm)	Soil depth (cm)	Fe (ppm)	Al (ppm)	Soil depth (cm)	Fe (ppm)	Al (ppm)	Soil depth (cm)	Fe (ppm)	Al (ppm)
2.5	2273	1298	2.5	3356	1861	2.5	13160	2577	2	1072	748	2.5	3004	756
7.5	2423	1317	7.5	3400	1879	7.5	17145	2937	7	102	222	7.5	1709	273
15	2307	1222	15	3039	2030	15	16408	2731	15	133	280	15	1583	230
30	2348	1174	35	3100	1942	30	4958	1470	25	189	431	30	761	180
65	3868	1605	80	2095	1156	50	4564	1017	43	4178	1330	50	497	115
									60	162	1914	76.5	568	139

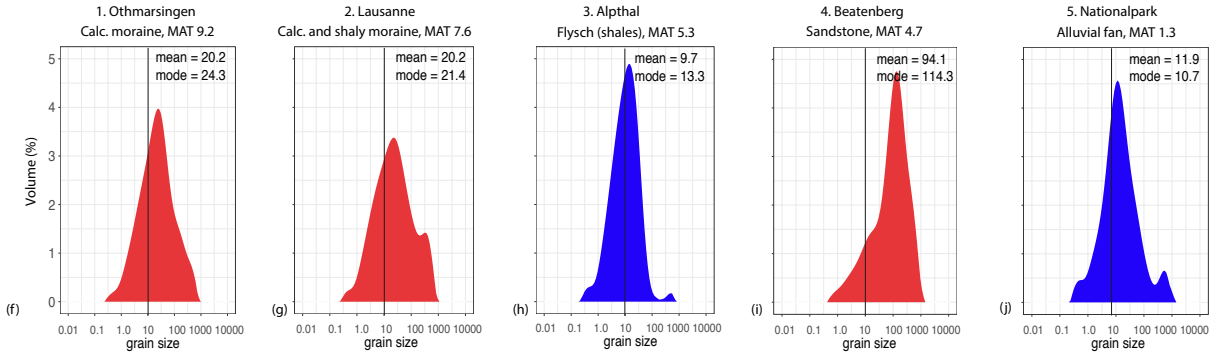

Figure S3 Visualization of grain size distribution five sites at 10-20 cm depth in the mineral soil. The sites Alptal and Nationalpark are underlain by respectively shale and intercalating alluvial fan with silty and sandy layers.

Table S8 Grain size distribution data of the five concerned sites.

Site	Depth	Grain size 0.1	Grain size mean	Grain size 0.9	Mode
Othmarsingen	2.5	3.1	19.8	151.0	21.4
	7.5	2.8	20.0	147.7	23.0
	15	2.6	20.2	157.0	24.3
	30	2.7	21.6	139.0	28.4
	50	3.0	30.2	217.0	38.0
	70	3.2	28.4	19.6	36.0
Lausanne	2.5	2.0	11.160	108.2	10.5
	7.5	2.4	17.3	150.7	19.1
	15	2.5	20.2	221.8	21.4
	30	2.2	16.5	198.5	17.7
	50	2.3	19.6	176.0	26.5
	70	2.6	22.2	253.9	25.7
Alptal	2.5	2.4	9.9	26.8	12.2
	7.5	2.5	12.3	36.6	16.9
	15	2.0	9.7	34.8	13.4
	30	1.9	8.3	27.0	10.6
Beatenberg	2.5	4.8	26.4	242.7	21.7
	15	7.3	94.1	384.5	114.3
	30	6.2	87.9	437.5	114.3
	50	7.3	75.9	296.9	112.8
Nationalpark	2.5	3.0	17.8	107.2	15.3
	7.5	1.7	9.5	87.7	8.9
	15	2.0	11.9	84.3	10.7
	30	3.0	22.8	706.1	623.6
	50	2.7	19.0	454.5	11.2
	70	3.4	36.9	857.7	690.0